Available online at www.sciencedirect.com
ScienceDirect
Journal of the European Ceramic Society 30 (2010) 2871–2880
www.elsevier.com/locate/jeurceramsoc

Porous alumina ceramics prepared with wheat flour

Eva Gregorová [a], Willi Pabst [a,*], Zuzana Živcová [a], Ivona Sedlářová [b], Svatava Holíková [a]

[a] *Institute of Chemical Technology, Prague (ICT Prague), Department of Glass and Ceramics, Technická 5, 166 28 Prague 6, Czech Republic*
[b] *Institute of Chemical Technology, Prague (ICT Prague), Department of Inorganic Technology, Technická 5, 166 28 Prague 6, Czech Republic*

Available online 18 April 2010

Abstract

It is shown that wheat flour can be used as a pore-forming and body-forming agent in ceramic technology. In contrast to pure native starch, however, the pores do not result from the swelling starch granules alone but are mainly due to protein-assisted foaming. Therefore the porosity is significantly higher and the pore size larger than that resulting from the starch granules alone, and the wet milling time applied for homogenizing the ceramic suspensions becomes the most critical process parameter. Alumina suspensions with 70 wt.% alumina and 20–30 vol.% wheat flour with different initial particle size (fine grade and semolina, respectively) have been prepared using milling times of up to 8 h. Porosities of up to approx. 60% can be achieved with only 20 vol.% of flour or semolina after 8 h of milling time, with the cell sizes (diameters of pore cavities resulting from foam bubbles) being essentially independent of the milling time (median diameters of 120–240 μm). Effective pore throat sizes (i.e. diameters of cell windows or channels between cells), measured via mercury porosimetry, are 1–2 μm for short milling times (2–3 h), but for long milling times (8 h) they change by more than one order of magnitude to median sizes of 20–30 μm, closely corresponding to the median size of wheat starch granules (approx. 20 μm).

Keywords: Milling (A); Microstructure-final (B); Porosity (B); Al_2O_3 (D); Starch consolidation casting

1. Introduction

Biopolymers of natural origin have been used in ceramic technology since the ancient times, e.g. straw in bricks and small plant fragments to increase the dry strength of pottery artifacts. In the second half of the 20th century, and mainly since its last decade, such biopolymers have been used as pore-forming agents in advanced fine ceramics to attain certain structural and/or functional properties as a result of controlled porosity, pore size and pore shape. For more than a decade now starch is one of the most popular pore-forming agents for this purpose.[1–27] Starch can be used as a mere pore-forming agent in combination with traditional shaping techniques, such as slip casting, or it maybe used as a combined pore-forming and body-forming (i.e. consolidating) agent in a process called starch consolidation or starch consolidation casting (SCC). The principles of this process are well known[1,2,5–8,18–26] and need not be repeated here. Among the advantages of starch are the well-defined product specification (including particle size distribution), easy processing, commercial availability and the complete burnout of starch without ash residues. Wheat starch is one of the less frequently used starch types in ceramic technology, which maybe partly due to the more bimodal particle size distribution[27–30] and partly due to the more anisometric (lenticular) shape of the large-size fraction (so-called A-fraction[29,30]). Moreover, wheat starch is a less common commodity on the world markets than other starch types.[31] On the other hand, however, wheat starch is a refined product of wheat flour, and the production volume of the latter exceeds the production of wheat starch (as well as other starch types) by orders of magnitude. Due to the significant added value in starch production, the price of flour is much lower than that of starch. Therefore wheat flour, which is produced simply by crushing and grinding (dry milling) wheat grains (endosperms), might intrude into ceramic market niches which are, for economic reasons, not accessible to wheat starch. This was the original motivation for this small study. After the first few tests, however, it became quite clear that the technological performance of flour in an SCC-type process, although very similar for the different flour grades (from fine to medium, coarse and very coarse, the latter grade being called semolina), is significantly different from that of starch.

Wheat flour consists of fragments of wheat (*Triticum aestivum* L.) grains, the inner part of which (representing the major

* Corresponding author.
E-mail addresses: eva.gregorova@vscht.cz (E. Gregorová), pabstw@vscht.cz, Willi.Pabst@vscht.cz (W. Pabst).

0955-2219/$ – see front matter © 2010 Elsevier Ltd. All rights reserved.
doi:10.1016/j.jeurceramsoc.2010.03.020

portion, viz. more than 80 wt.%) is called the endosperm.[28,32] The flour grade (fine, medium, coarse, or very coarse, i.e. semolina) is essentially a result of a crushing and grinding (dry milling) process performed on a large industrial scale. Wheat endosperms are composed of starch granules, occupying 63–72 vol.% of the endosperm (large, lenticular ones, so-called A-starch, and small, spherical ones, so-called B-starch, both consisting of amylose and amylopectin[29–31]), embedded in a porous protein matrix (6–20 vol.% protein, mainly gluten, the rest being porosity).[32] In small amounts the protein matrix contains the enzyme amylase (β-amylase), which is able to decompose the polysaccharides amylose and amylopectin in aqueous environments into fermentable lower saccharides (mainly the disaccharide maltose), which may produce gases during fermentation.[33]

Thus, in contrast to pure refined wheat starch, both the protein content and the fermentation-related gas release in wheat flour can be expected to be foster bubble formation (foaming) and thus modify the SCC process considerably. For this reason it was deemed necessary to perform a more complex study, not only concerning the determination of chemical composition, ash content and burnout characteristics (Section 2), particle size characterization, suspension rheology and swelling kinetics (Section 3), but also dealing in some detail with the microstructural characterization of the resulting porous ceramics after firing (Section 4). The results of the present study show that flour, when used in an SCC-type process, is indeed a unique pore-forming and processing agent and that microstructures can be obtained that are unattainable with pure native starch alone. The reasons for this difference will be discussed (Section 5).

2. Experimental

In this work the following pore-formers have been used: wheat starch (Pšeničný škrob, Škrobárna Havlíčkův Brod s.r.o., Czech Republic), fine flour (Předměřická mouka pšeničná – hladká, Mlýny Voženílek s.r.o., Czech Republic) and very coarse flour (semolina, Zátkova jemná krupička, Bratři Zátkoví a.s., Czech Republic). The composition of these pore-formers (in wt.% of elements or oxides) have been determined by X-ray fluorescence analysis (XRF, ARL 9400 XP, Switzerland), their burnout behavior using thermogravimetry and differential thermal analysis/DTA (Setys Evolution 1750, Setaram, France), and the gases evolving during burnout have been analyzed by mass spectrometry (OmniStar TM, Pfeiffer Vakuum, Germany). Particle size distributions have been measured by laser diffraction (Particle Sizer Analysette 22 Nanotec, Fritsch, Germany) using the Fraunhofer approximation for data evaluation.

Alumina suspensions containing flour and semolina, respectively, were prepared with 70 wt.% of submicron alumina (CT-3000 SG, Almatis, Germany) in distilled water, adding 1 wt.% (related to alumina, density 4.0 g/cm^3) of deflocculant (Dolapix CE 64, Zschimmer & Schwarz, Germany) and 20 vol.% (nominally, i.e. related to solids alone) of flour and semolina (density 1.5 g/cm^3), respectively. After mixing, the suspensions underwent wet ball milling (homogenization) for 2, 3 or 8 h in polyethylene bottles (100 cm^3) with 4 alumina balls (diameter 1 cm), using a laboratory shaker (HS 260, IKA, Germany) at a frequency of 5 Hz. Viscometric measurements of the as-prepared (bubbly) suspensions after ball milling were made on a rotational viscometer (RV1, ThermoHaake, Germany) with a coaxial cylinder system (Z41).

SCC processing was performed in the same way as for pure native starch (described elsewhere in greater detail[23]), i.e. casting into metal molds, heating to 80 °C for 2 h, followed by overnight cooling, demolding and subsequent drying at ambient temperature for 24 h and final drying at 105 °C for approx. 2 h. The as-dried samples were fired in an electrofurnace under air at 1570 °C, using a conventional firing schedule (heating rate 2 °C/min, dwell time at maximum temperature 2 h).

Bulk density and total porosity of the samples after firing were determined by the Archimedes method (weighing of dry and water-saturated bodies in water—after boiling in water for 2 h and subsequent cooling in water for 24 h) and mercury porosimetry (AutoPore IV 9500, Micromeritics, USA), operated up to maximum pressures of 400 MPa. Mercury porosimetry was also used for determining the "pore size" distribution (more precisely, the cell window[34] or pore throat/interconnecting channel diameter distribution) according to the Washburn equation (i.e. the equivalent cylinder model).[35] Linear shrinkage was measured by a slide caliper on cylindrical samples with diameter approx. 8 mm.

The cell size[34] (or pore cavity diameter) distribution was determined via microscopic image analysis, performed based on micrographs from an optical microscope (Jenapol, Zeiss, Germany) by marking manually approx. 1000 objects per sample via their area-equivalent circles and evaluating via an image analyzing software (Lucia Version 4.81, Laboratory Imaging, Czech Republic). For comparison, a Saltykov transformation[36] has been applied to correct for the random section problem, although this correction is not essential to the results of the present paper. In order to compare the (number-weighted) image analysis results with the (volume-weighted) laser diffraction and mercury porosimetry results, the image analysis results have been transformed under the assumption of a size-invariant pore shape (the exact procedure has been described elsewhere[37]).

3. Results

3.1. Composition, ash content and burnout characteristics

The first part of Table 1 (first 4 lines) shows the elemental composition of wheat starch, fine flour and semolina, as determined by X-ray fluorescence analysis. Taking into account that the dominant constituent is of organic character, with elements that cannot be determined using this method (C, O and H), these are only relative values. Therefore, it seems reasonable to renormalize these results with respect to the ash contents after complete burnout of the organics at a temperature of 800 °C; these are 0.03, 1.1 and 6.8 wt.% for native wheat starch, fine flour and semolina, respectively (cf. also Fig. 1). The second part of Table 1 (lines 5–9) shows the renormalized elemental compositions and the third part of Table 1 (lines 10–14) the renormalized compositions transformed to equivalent oxide contents.

Table 1
X-ray fluorescence (XRF) analyses of wheat-based products (top table: relative concentrations of elements, middle table: absolute concentrations of elements, renormalized with respect to the total ash content after burnout to 800 °C, bottom table: absolute concentrations of oxides, renormalized with respect to the total ash content after burnout to 800 °C; all values in wt.%).

	Na	Mg	Al	Si	P	S	Cl	K	Ca
Semolina	<0.009	0.025	0.013	0.009	0.100	0.170	0.063	0.132	0.015
Fine flour	–	0.040	<0.003	0.001	0.146	0.203	0.068	0.173	0.023
Wheat starch	0.044	0.008	0.097	0.062	0.059	<0.005	0.012	0.029	<0.009
	Na	Mg	Al	Si	P	S	Cl	K	Ca
Elements, renormalized with respect to the total ash content after burnout to 800 °C									
Semolina	–	0.271	0.139	0.097	1.120	2.060	0.843	1.950	0.265
Fine flour	–	0.071	–	–	0.261	0.365	0.122	0.315	0.043
Wheat starch	<0.01	–	<0.01	<0.01	<0.01	–	–	–	–
	Na_2O	MgO	Al_2O_3	SiO_2	P_2O_5	SO_3	Cl	K_2O	CaO
Oxides, renormalized with respect to the total ash content after burnout to 800 °C									
Semolina	–	0.347	0.202	0.160	1.950	1.540	0.614	1.680	0.254
Fine flour	–	0.085	–	–	0.431	0.262	0.087	0.269	0.043
Wheat starch	–	–	<0.01	<0.01	<0.01	–	–	–	–

It is evident that starch is virtually free of contaminants, while fine flour and especially semolina contain significant amounts mainly of P, S, Cl and K (from salt contents in the wheat grain) and – to a lesser but clearly non-negligible amount – Mg, Ca, Al, Si (from the industrial grinding media). Therefore the ash composition can be expected to consist of potassium and earth alkaline salts (chloride, sulfates and phosphates), with a small amount of alumina and silica. Fig. 1 shows the thermogravimetric curves of starch, fine flour and semolina. The burnout behavior of the three materials looks quite similar, beginning (after a drying step at low temperature to eliminate hygroscopically bound water) at approx. 250 °C with a steep decrease (mainly caused by dehydroxylization, i.e. elimination of OH groups) and ending at approx. 550 °C with the complete elimination of the organic constituents (elements C and H). This behavior is very similar not only to wheat starch but to other starch types as well.[23,26] Fig. 2 shows the corresponding DTA curves. In contrast to wheat starch (and other starch types as well[23,26]) the strongly endothermic peak at 300 °C is not present in fine flour and semolina. The mass-spectrometric analysis of gases shown in Fig. 3 indicates that this peak corresponds primarily to dehydroxylization (destruction of OH groups in the starch polysaccharides). Denitrification (i.e. the elimination of nitrogen-containing groups in the starch polysaccharides and the proteins) and decarbonization reactions start at this temper-

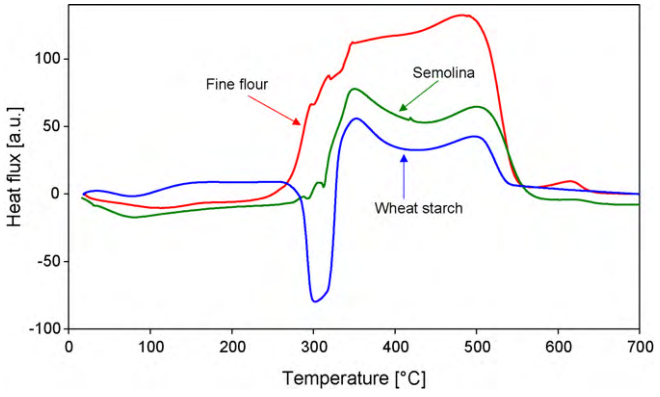

Fig. 2. DTA curves of wheat starch (in the center of the bottom curve), fine flour (top curve), and semolina (intermediate curve).

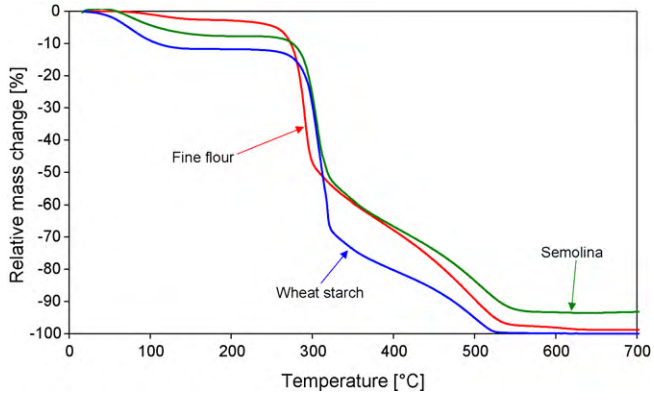

Fig. 1. Thermogravimetric curves of wheat starch (on the r.h.s. the bottom curve), fine flour (intermediate curve), and semolina (top curve).

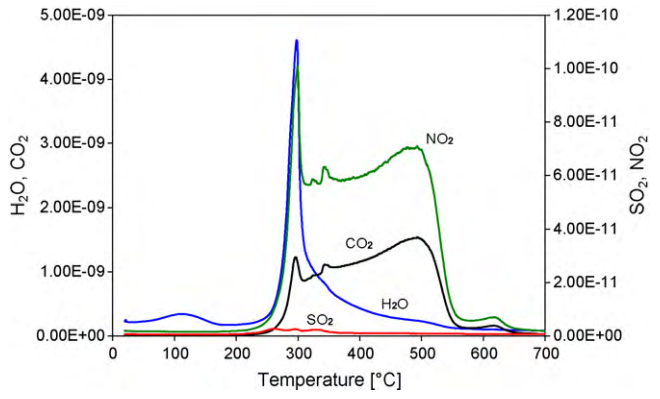

Fig. 3. Mass-spectrometric analysis of gases evolving during burnout of fine flour (from top to bottom H_2O, NO_2, CO_2, and SO_2).

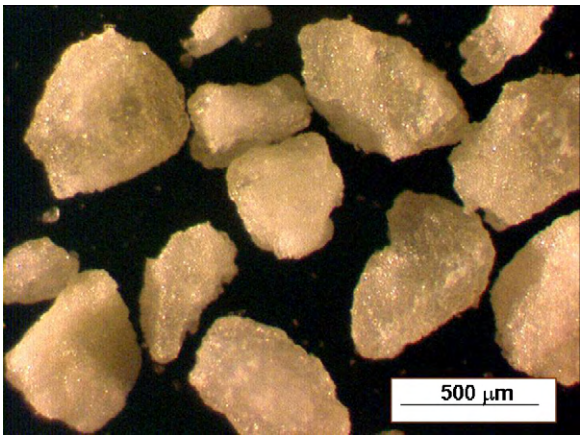

Fig. 4. Dry semolina (optical micrograph illuminated from above).

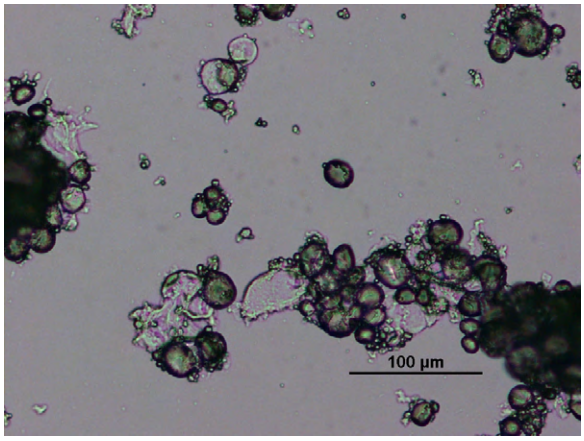

Fig. 6. Fine flour in water (optical micrograph illuminated from below).

ature as well, but these have a second maximum at significantly higher temperatures (approx. 500 °C), at which OH groups are not present any more. Mass-spectrometric analyses of gases evolving due to starch burnout are very similar (except for the absence of sulfur oxides),[23] and the reason why the endothermic peak typical for starches is missing in the DTA curves of fine flour and semolina is far from being clear.

3.2. Particle characterization, suspension rheology and swelling kinetics

Figs. 4–7 show optical micrographs of dry semolina, semolina in water, fine flour and native wheat starch, respectively. It can be seen that semolina consists of large agglomerates of starch granules (Fig. 4). In the dry state they are relatively hard, stiff and strong, but in water (even in cold water at approx. 20 °C) they readily disintegrate into starch granules (see Fig. 5). The detailed micrograph of fine flour (Fig. 6) shows that apart from smaller agglomerates and individual starch granules there are flaky constituents representing non-starch components of the wheat endosperm. Native wheat starch (Fig. 7) is a bimodal mixture of coarse A-starch (lenticular) and fine B-starch (spherical).[20,27] Figs. 8 and 9 show the particle size distributions of fine flour and semolina, as measured by laser diffraction

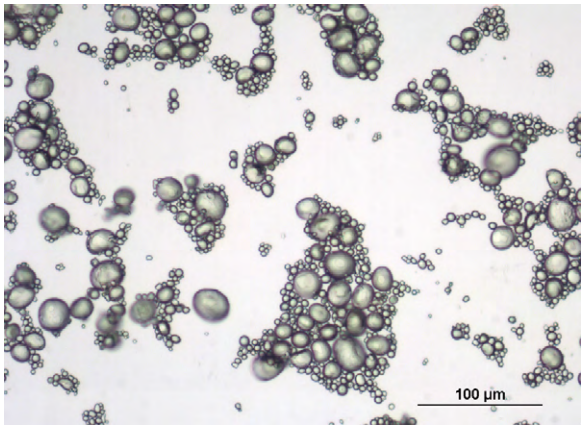

Fig. 7. Native wheat starch in water (optical micrograph illuminated from below).

immediately after mixing in water at 20 °C (full curves) and after 4 h soaking in water at 20 °C (dashed curves), respectively. For fine flour (Fig. 8) there is almost no difference and the size distribution is similar to that of native wheat starch (median diameter approx. 18–21 μm, mode approx. 23 μm), cf. Ref.[27] For semolina (Fig. 9), the initial size distribution is bimodal, exhibiting a second mode at approx. 500 μm. However, the

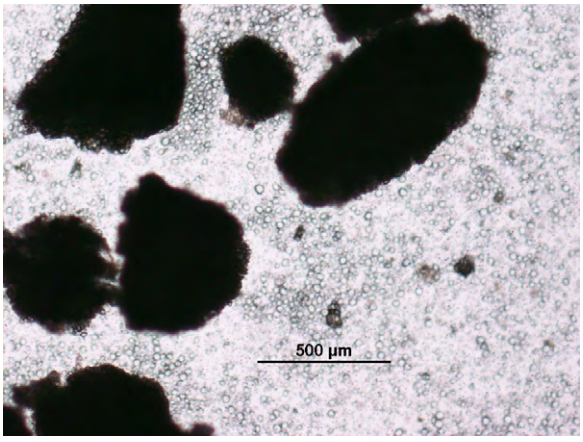

Fig. 5. Semolina in water (optical micrograph illuminated from below).

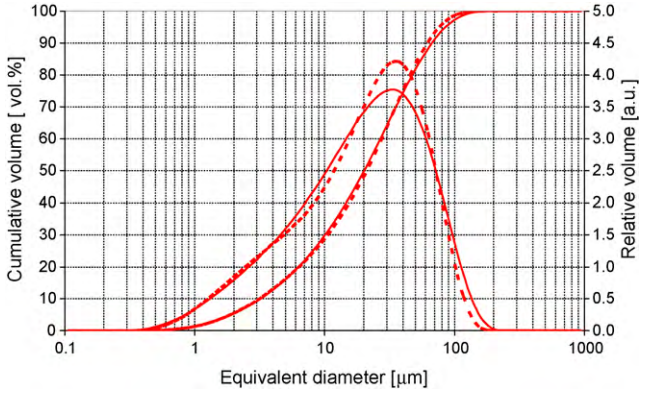

Fig. 8. Particle size distribution of fine flour, measured via laser diffraction (full curve immediately after mixing, dashed curve after 4 h soaking in water at 20 °C).

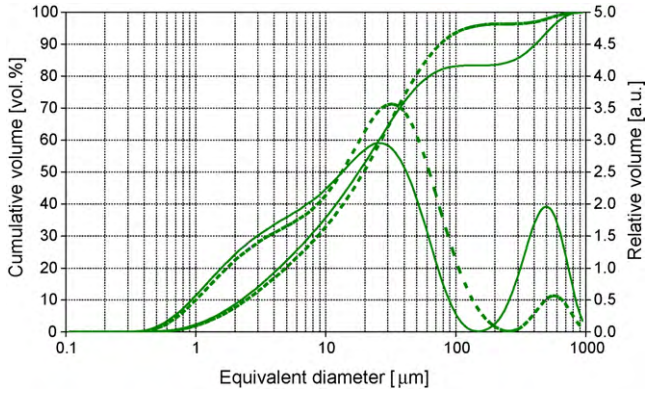

Fig. 9. Particle size distribution of semolina, measured via laser diffraction (full curve immediately after mixing, dashed curve after 4 h soaking in water at 20 °C).

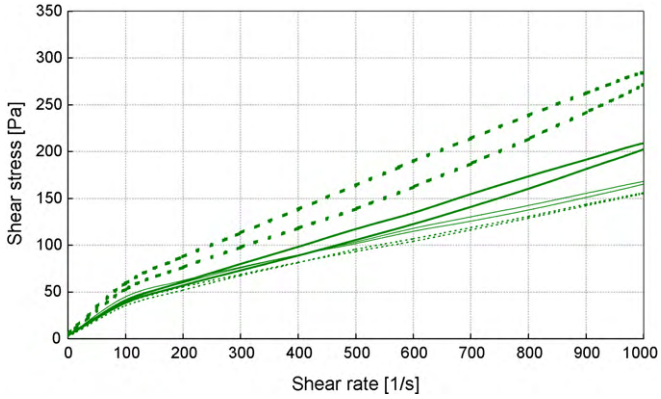

Fig. 11. Flow curves of alumina suspensions with semolina; from bottom to top: A70F20-2h (thin full), A70F20-3h (thick dotted), A70F30-2h (thick full), A70F30-3h (thick dotted); yield stress 3.5 ± 1.1 Pa.

agglomerates are relatively easily disrupted: after 4 h soaking in cold (20 °C) water the ultrasonication standardly applied in the laser granulometer is able to deagglomerate a substantial part of the agglomerates, so that the relative amount of the large-size fraction is significantly decreased. The median diameters are not influenced too much even in the latter case. They are 20–21 μm for fine flour and 18–20 μm for semolina, i.e. very close to the median diameter of native wheat starch.

Particle size distributions of alumina suspensions containing flour and semolina, respectively, measured after 2 h wet milling confirm these findings: all flour and semolina agglomerates have disappeared and the overall particle size distributions of the two suspensions are more or less identical (microstructural investigations, however, showed that 2 h of wet milling is too short for this system to eliminate all alumina agglomerates).

Figs. 10 and 11 show the flow curves of 70 wt.% alumina suspensions with 20 vol.% (bottom curves, thin) and 30 vol.% (top curves, thick) of flour and semolina, respectively, after 2 h (full) and 3 h (dotted) of wet milling. It is evident that the rheological character is shear-thinning with a tendency to stronger thixotropy for higher concentration and longer milling times. The apparent viscosities, however, are relatively low (below 500 mPa s at a shear rate of 500 s^{-1}), ensuring sufficient fluidity for casting and a reasonable potential for future rheological-concentrational optimization. Yield stresses are negligibly small (approx. 3.5 Pa), but may increase with an increasing content of gas bubbles. Of course, when process optimization is required, both yield stresses and apparent viscosities maybe controlled by the type and content of deflocculants and other additives (e.g. defoamers).

Figs. 12 and 13 show the swelling kinetics of flour and semolina in water when heated up to 80 °C. The method has been used for native starch previously and is described elsewhere.[23,26] After heating for precisely defined times the samples were quenched by injecting the suspensions into the measuring cell of a laser diffraction granulometer. Note that the arithmetic mean diameter (and not the median diameter) of the volume-weighted distribution is commonly used as a characteristic size measure in this case, because only the former allows a transformation of the values to volumetric swelling values.[6,23,26,38] We note in passing that for bimodal size distributions the arithmetic mean diameter can be significantly different from the median (in our case the median diameter for semolina is approx. 30 μm, while the arithmetic mean diameter is approx. 130 μm). Apart from the initial stage of agglomerate swelling of the semolina grains (Fig. 13) the swelling kinetics of both fine flour and semolina (after disintegration of the agglomerates) is very similar to that of pure

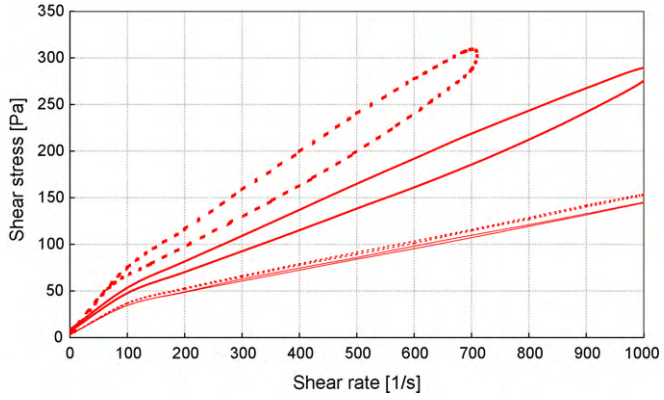

Fig. 10. Flow curves of alumina suspensions with fine flour; from bottom to top: A70F20-2h (thin full), A70F20-3h (thick dotted), A70F30-2h (thick full), A70F30-3h (thick dotted); yield stress approx. 3.5 ± 1.8 Pa.

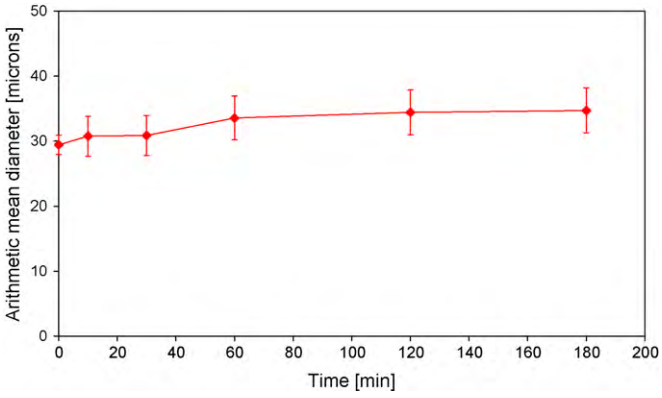

Fig. 12. Swelling kinetics of fine flour in water at 80 °C (arithmetic mean diameters from laser diffraction, error bars indicate the combined effect of sample-to-sample variation and size uncertainty during swelling).

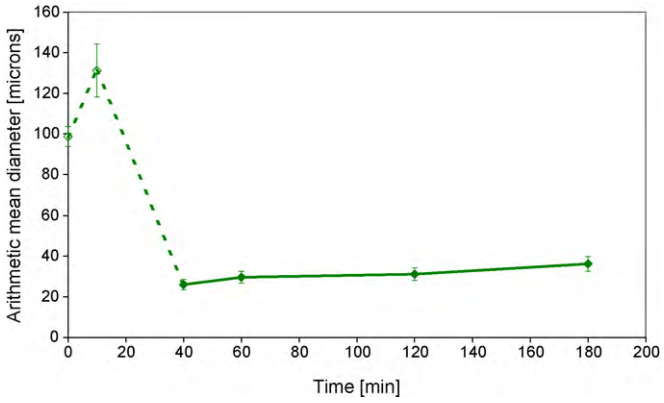

Fig. 13. Swelling kinetics of semolina in water at 80 °C (arithmetic mean diameters from laser diffraction, error bars indicate the combined effect of sample-to-sample variation and size uncertainty during swelling).

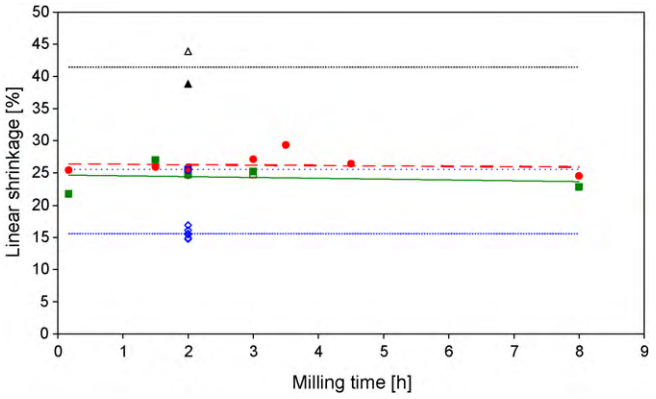

Fig. 14. Linear shrinkage of porous alumina ceramics prepared from 70 wt.% alumina suspensions with fine flour (circles, full with 20 vol.% flour – A70F20, empty with 30 vol.% flour – A70F30) or semolina (squares, full with 20 vol.% semolina – A70S20, empty with 30 vol.% semolina – A70S30) as well as 50 wt.% alumina suspensions with 50 vol.% of fine flour (full triangle – A50F50) or 50 vol.% (empty triangle – A50S50); trend lines obtained by linear regression (dashed – fine flour, full – semolina); dotted lines (from top to bottom): alumina suspensions with 50, 70 and 80 wt.% alumina, respectively (diamonds denote previous results with pure native wheat starch,[39] shown for comparison).

native starch.[6,23,26] From this point of view, therefore, virtually all wheat flour grades (from fine flour to semolina) can be used as potential substitutes of native starch in the SCC process. The swelling factor of flour and semolina, however, is significantly lower than for pure starch (approx. 1.2–1.4, compared to 1.9 for starch[26]).

3.3. Microstructural characterization of porous alumina ceramics

Table 2 lists values of bulk density, porosity and shrinkage in dependence of the milling time for porous alumina ceramics prepared from alumina suspensions with 70 wt.% alumina and flour or semolina contents of 20 and 30 vol.% (nominally). We use the following self-explanatory notation: A70F20, A70F30, A70S20, A70S30 and add the milling time wherever necessary (−2, −3 and −8 h). For reasons of comparison, higher contents of flour and semolina have been tested as well (50 vol.% nominally), with milling times of 2 h (i.e. A50F50-2h and A50S50-2h). In this case the alumina concentration in the suspension was reduced to only 50 wt.% to ensure sufficient fluidity for casting.

Despite the great scatter of measured values (each data point is an average of 5–10 specimens), which indicates a great batch-to-batch variability especially for short milling times, there is a clear trend towards lower bulk density (higher porosity) for longer milling times. Porosities of up to 60% can be achieved with a nominal flour or semolina content of only 20 vol.%, cf. Table 2 (note that with this content the resulting porosity would be only approx. 20% if flour or semolina would act merely as sacrificial pore-formers). Most remarkably, the influence of the milling time seems to override completely even very pronounced compositional differences (concerning concentration and flour grade). This can be seen by considering the bulk density and porosity values for the porous alumina samples prepared from 50 wt.% alumina suspensions with 50 vol.% of flour or semolina (A50F50-2h and A50S50-2h): within the scatter of measured values (batch-to-batch variations) the values lie in the same range as for the A70 samples with 20 or 30 vol.% flour or semolina.

Fig. 14 shows that shrinkage is more or less independent of the milling time and even on the content of flour or semolina in the suspensions. It is essentially a function only of the alumina content in the suspensions and is approx. 25 ± 2% for a 70 wt.% alumina suspension, cf. Table 2. This finding is in accordance with the results of earlier work with pure native wheat starch,[39] cf. the empty diamond symbols in Fig. 14. For reasons of com-

Table 2
Characteristic microstructural parameters (ϕ_{open} = open porosity, ϕ = total porosity, σ = linear shrinkage).

Sample	Milling time [h]	Archimedes			σ	Mercury porosimetry		
		Bulk density [g/cm^3]	ϕ_{open} [%]	ϕ [%]		Bulk density [g/cm^3]	ϕ_{open} [%]	ϕ [%]
A70F20	2	2.47	29.4	38.2	24.6	2.511	30.9	37.2
A70F20	3	2.03	40.6	49.4	27.6	2.046	47.6	48.9
A70F20	**8**	1.64	57.2	59.1	24.5	2.522	55.7	37.0
A70F30	2	2.78	21.7	30.5	25.5	2.658	27.7	33.6
A70F30	3	2.35	30.5	41.3	24.7	2.292	38.9	42.7
A70S20	2	2.62	21.5	34.4	24.7	2.651	28.4	33.7
A70S20	3	2.62	16.9	34.5	25.2	2.620	28.0	34.5
A70S20	**8**	1.49	55.6	62.7	22.8	2.620	57.2	34.5
A70S30	2	2.76	21.6	30.9	25.2	2.689	27.3	32.8
A70S30	3	1.98	45.6	50.5	24.8	1.977	42.1	50.6

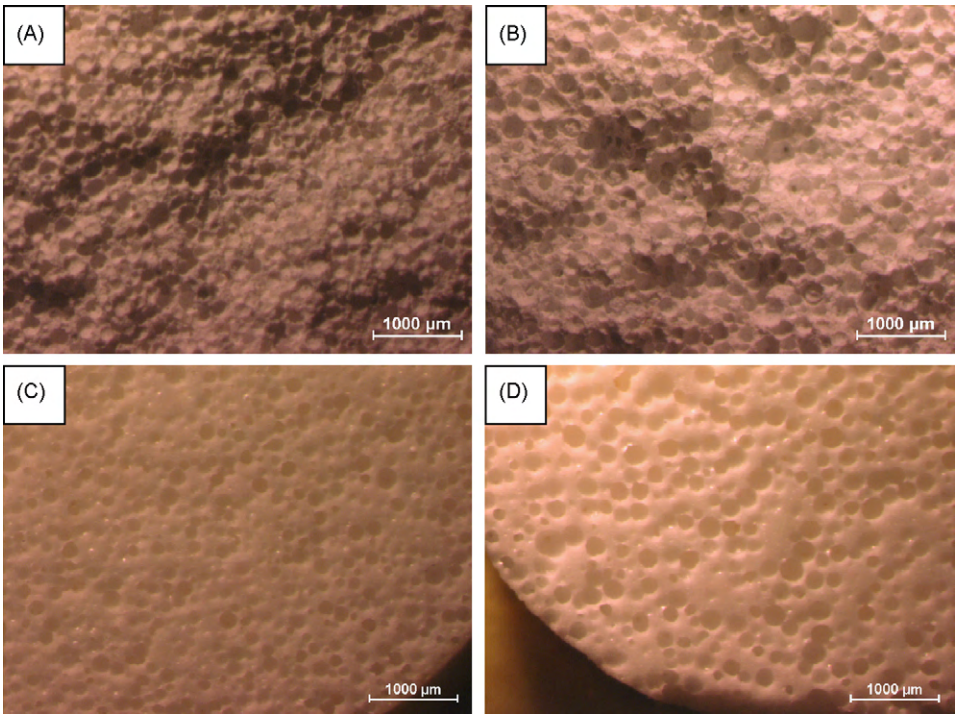

Fig. 15. Microstructure of as-dried green bodies (fracture surfaces: a and b) and as-fired bodies (diamond-cut sections: c and d) of porous alumina prepared from 70 wt.% alumina suspensions with 20 vol.% of fine flour (a and c; 8 h wet milling – A70F20-8h) and semolina (b and d; 8 h wet milling – A70S20-8h).

parison the average shrinkage is also shown for 50 and 80 wt.% alumina suspensions, respectively.

Fig. 15a and b shows the microstructures (fracture surfaces) of porous alumina green bodies (A70F20-8h and A70S20-8h) after drying, while Figs. 15c, 15d and 16 show the corresponding microstructures after firing. Obviously, the microstructure is in both cases very similar, corresponding to the fact that also the microstructural parameters (bulk density and porosity in Table 2) are rather close. It has to be emphasized that only after 8 h of milling the microstructures are homogeneous and well reproducible. With shorter milling times (2–3 h) the batch-to-batch variation is quite large and the process controllability is only moderate. Moreover, alumina agglomerates are not completely disrupted by such short milling times, when flour or semolina is used as a processing additive (in contrast to the case when pure native starch is used).

Fig. 17 shows the "pore size" distributions of the porous alumina ceramics prepared, measured by microscopic image analysis (after transformation to volume-weighted distributions[37,40]) and mercury porosimetry (cell window sizes or effective pore throat diameters). It is evident, that the image analysis results are much larger than the mercury porosimetry results, as expected. As mentioned before, the former method

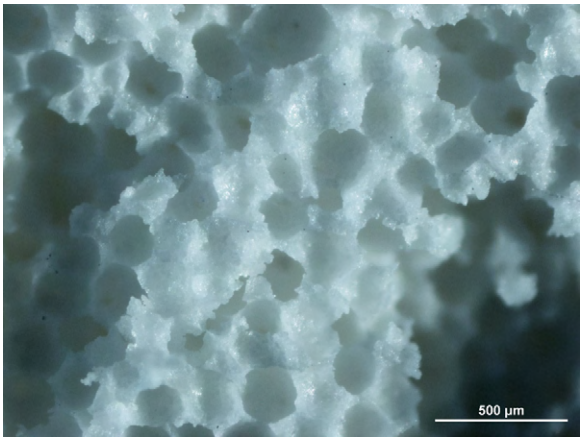

Fig. 16. Microstructure of as-fired porous alumina prepared from a 70 wt.% alumina suspension with 20 vol.% of semolina (8 h wet milling – A70F20-8h); fracture surface (detail).

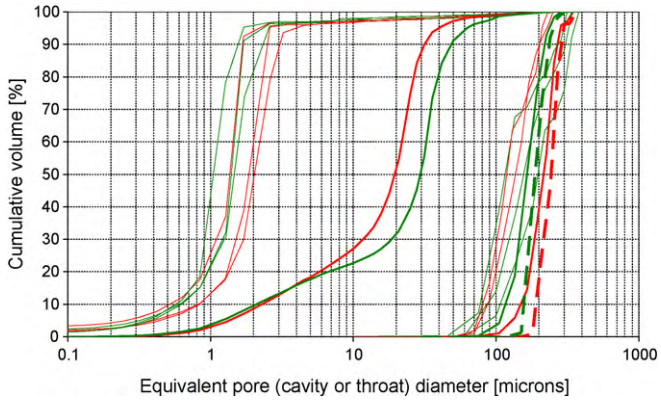

Fig. 17. Pore size distributions of porous alumina ceramics measured by microscopic image analysis (bundle of nine curves on the r.h.s., after transformation to volume-weighted distributions[37,40]) and mercury porosimetry (two curves in the middle and on the l.h.s.); thin curves are for milling times 2–3 h (not distinguished), thick curves for milling times 8 h (thick full curves without Saltykov transformation, thick dotted curves with Saltykov transformation[36]); there is no systematic difference between materials prepared with fine flour or with semolina.

Table 3
Characteristic parameters of the pore size distribution (minimum and maximum median values are boldface).

Sample	Milling time [h]	Mercury porosimetry			Image analysis		
		D_{10} [μm]	D_{50} [μm]	D_{90} [μm]	D_{10} [μm]	D_{50} [μm]	D_{90} [μm]
A70F20	2	0.8	**2.1**	3.1	–	–	–
A70F20	3	–	–	–	–	–	–
A70F20	8	2.3	**19.5**	31.5	149	216	270
	Saltykov			191	**243**	287	
A70F30	2	0.6	1.5	1.7	81	119	202
A70F30	3	0.8	1.7	2.5	87	137	202
A70S20	2	0.6	1.5	2.4	77	**117**	273
A70S20	3	0.6	**1.1**	1.6	–	–	–
A70S20	8	2.1	**29.4**	48.7	117	164	220
	Saltykov			157	188	237	
A70S30	2	0.6	1.5	1.7	108	197	334
A70S30	3	–	–	–	89	157	307
			Laser diffraction			Image analysis	
	Wheat starch	3.2	17.7	9.9	10.4	18.0	25.7

measures the cell sizes (diameters of the large pore cavities), while the latter measures essentially the window cells (pore throat diameters, i.e. effective diameters of the interconnections between pore cavities), since the standard evaluation of measured data via the Washburn relation is based on equivalent cylinder pore geometry.[35] The difference for short milling times, however, is by two orders or magnitude, which is rather unusual. When pure native starch is used, the difference is only about one order of magnitude.[23,34] The cell window size (pore throat diameter) measured here corresponds to that in porous ceramics prepared with pure native starch.[23,34] That means, the large pore cavities (cells with median diameters 120–240 μm) are usually embedded in a matrix containing medium-sized pores (cells with medium diameters 20–29 μm, i.e. residual pores resulting from burnout of individual wheat starch granules), which are by themselves connected via small windows (with median diameters 1–2 μm), cf. Table 3. Only when the porosity becomes very high (due to excessive foaming) the foam bubbles get in direct contact (without the mediating small windows) and the medium-sized residual pores (cells) from starch burnout now by themselves take over the role of the connecting channels or "effective pore throats" (thick curves in the middle of Fig. 17). Fig. 18 confirms this hypothesis, because the particle size of wheat starch is remarkably close to that of the medium-sized pore channels (the laser diffraction results even copy the shape of the distribution curve determined by mercury porosimetry).

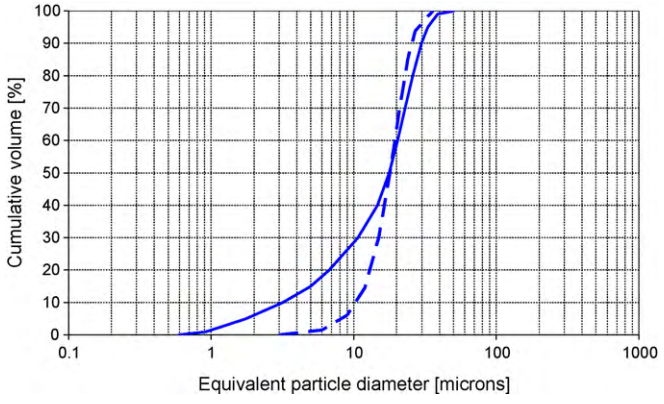

Fig. 18. Particle size distribution of wheat starch measured by image analysis (dashed curve, after transformation to a volume-weighted distribution[37,40]) and laser diffraction (full curve).

This explains also the incorrect porosity values determined by mercury porosimetry after 8 h of milling (cf. Table 2): since the bulk density is determined at atmospheric pressure (0.1 MPa), where pores (pore channels) with a diameter larger than approx. 15 μm are already filled (in accordance with the Washburn equation[35]), the resulting bulk density value is expectedly too high, and thus the total porosity (calculated using the theoretical density of alumina) is too low. We note in passing that – within experimental scatter – there is no systematic difference between ceramics prepared with fine flour or semolina, neither between ceramics prepared with 20 or 30 vol.% of these additives. In other words, the milling time seems to be the main relevant parameter for controlling the effective pore throat size (which can be either 1–2 or 20–30 μm, depending on the milling time chosen). Interestingly, milling time seems to have a negligible influence on the size of the large pore cavities (cell size).

4. Discussion

The results clearly indicate that during the homogenization of the ceramic suspensions by wet milling the wheat grain fragments are disintegrated and after milling the particle size is more or less that of starch granules (essentially the coarse size fraction, i.e. A-starch). Therefore the technological behavior of the ceramic suspensions is more or less independent of the flour grade used. Moreover, it is evident that fine flour and semolina (and of course any intermediate flour grade) lead to very similar microstructures in the as-fired ceramics when a SCC-type process is used. The most significant difference to SCC with pure native starch is the presence of large pores that are not a result of starch burnout (neither of flour or semolina particles, of course, since these are not present after wet milling any more, in contrast to the procedure used in Ref.[41]), but which are essentially foam bubbles solidified during drying and firing. Pores of that

kind (with median diameters of 120–240 μm) are not known from SCC with pure native starch and must therefore be a typical feature of flour and semolina, more precisely of the protein content of these wheat grain products (cf. Section 1). This conclusion is in accordance with the fact these large pores are not only uninfluenced by the flour grade used, but also rather insensitive to the flour or semolina concentration in the suspensions. Proteins are well-known foam-formers.[42] In particular, they can be foamed by mechanical agitation (stirring), a well-known feature which is exploited in the preparation of ceramic foams from egg white, cf. Ref.[42] This foaming ability can be enhanced in water and influenced by additions of salts and other ingredients, and powders (including starch granules) may act as foam stabilizers in such systems.[43] In particular, the small-size fraction of starch (so-called B-starch) maybe expected to take over this function. The findings of our study, however, in particular the obvious dependence on the results on milling time, indicate that additionally the enzymatic decomposition of the starch polysaccharides (amylose and amylopectin) into fermentable saccharides (mainly maltose) by amylase[33] and their subsequent fermentation play a non-negligible role in that the gases developed after 8 h of milling contribute significantly to foaming. As a result, porous alumina ceramics prepared with flour (any grade) may attain 60% porosity although only 20 vol.% of flour (nominally, i.e. related to alumina) has been used. Comparable results cannot be achieved by SCC with pure native starch. Moreover, the relatively low content of flour required for attaining quite high porosity may significantly decrease the contamination of the ceramics due to the residual ash content mentioned in Section 3.1. In other words, the higher ash content in flour and semolina is partly compensated by the fact that less flour than starch is needed to attain a required porosity. Further optimization may lead to the selection of flour types and/or grades with even lower ash content, so that the contamination problem may in the end turn out to be less severe in practice than it may appear from the findings in Section 3.1. Nevertheless, one should be very cautious to apply flour in applications requiring high purity and it should not be forgotten that the microstructure of the resulting ceramics is completely different. In particular, the pore sizes obtained with SCC using pure native starch are completely different from those obtained when flour is used in a SCC-type process (much larger pore cavities or cells). In ceramic technology in general, wet milling of ceramic suspensions is an indispensible processing step to obtain homogenized and agglomerate-free, low-viscosity slurries. Previous tests related to the work have clearly shown that a milling time of 2 h is too short for this purpose when flour or semolina is used (in contrast to pure native starch). The probable reason is that a substantial part of the milling energy is consumed in cracking the agglomerates of flour or semolina and is therefore not disposable for the deagglomeration of the submicron alumina agglomerates. After 8 h of milling the homogenization of the suspensions is very good, while the additional foaming effect is not accompanied by pore growth. Thus the wet milling time can be used as a parameter for porosity control, and possibly even higher porosities could be achieved simply by increasing the milling time.

5. Conclusion

In this contribution it has been shown that wheat flour, i.e. crushed and ground (dry milled) fragments of wheat grains (endosperms), can be used as a pore-forming and body-forming agent in ceramic technology. These materials, which are composed essentially of starch granules in a protein matrix, are much cheaper than pure native starch and might therefore intrude into ceramic market niches inaccessible to starch. The technological behavior of different flour grades (size classes) is similar, with characteristic differences to pure native starch, and their starch content allows an SCC-type process (i.e. a process analogous to starch consolidation casting) to be applied, enabling casting of ceramic suspensions into metal molds. In contrast to pure native starch, the pores in the ceramic do not result from the swelling (and gelatinizing) starch granules alone, but are mainly due to protein-assisted foaming, resulting in foam bubbles (after wet milling), probably stabilized by starch granules. Therefore the porosity is significantly higher and the pore size significantly larger than that resulting from the starch granules alone, and the wet milling time applied for homogenizing the ceramic suspensions becomes the most critical process parameter. Alumina suspensions with 70 wt.% alumina and 20–30 vol.% (related to alumina) wheat flour with different initial particle size (fine grade and semolina, respectively) have been prepared using milling times of up to 8 h. Porosities of up to approx. 60% can be achieved with only 20 vol.% of flour or semolina after 8 h of milling time, with the sizes of pore cavities or cells (essentially foam bubbles), as measured by microscopic image analysis, being essentially insensitive to the milling time (median diameters of 120–240 μm). Effective pore throat sizes (i.e. diameters of cell windows or channels between cells), measured via mercury porosimetry, are 1–2 μm for short milling times (2–3 h), but for long milling times (8 h) they change by more than one order of magnitude to median sizes of 20–30 μm, closely corresponding to the median size of wheat starch granules (approx. 20 μm).

Acknowledgements

This study was part of the project IAA401250703 “Porous ceramics, ceramic composites and nanoceramics“, supported by the Grant Agency of the Academy of Sciences of the Czech Republic and of the frame research programme MSM 6046137302 “Preparation and research of functional materials and material technologies using micro- and nanoscopic methods“, supported by the Ministry of Education, Youth and Sports of the Czech Republic. Support is gratefully acknowledged. Moreover, the authors would like to thank Dr. S. Randáková (Central Laboratories of the ICT Prague) for the XRF measurements.

References

1. Lyckfeldt O, Ferreira JMF. Processing of porous ceramics by “starch consolidation”. *J Eur Ceram Soc* 1998;**18**:131–40.

2. Alves HM, Tarí G, Fonseca AT, Ferreira JMF. Processing of porous cordierite bodies by starch consolidation. *Mater Res Bull* 1998;**33**:1439–48.
3. Corbin SF, Apte PS. Engineered porosity via tape casting, lamination and the percolation threshold of pyrolyzable particulates. *J Am Ceram Soc* 1999;**82**:1693–701.
4. Davis J, Kristoffersson A, Carlström E, Clegg W. Fabrication and crack deflection in ceramic laminates with porous interlayers. *J Am Ceram Soc* 2000;**83**:2369–74.
5. Lemos AF, Ferreira JMF. Porous bioactive calcium carbonate implants processed by starch consolidation. *Mater Sci Eng* 2000;**C11**:35–40.
6. Pabst W, Týnová E, Mikač J, Gregorová E, Havrda J. A model for the body formation in starch consolidation casting. *J Mater Sci Lett* 2002;**21**:1101–3.
7. Týnová E, Pabst W, Gregorová E, Havrda J. Starch consolidation casting of alumina ceramics—body formation and microstructural characterization. *Key Eng Mater* 2002;**206–213**:1969–72.
8. Bowden ME, Rippey MS. Porous ceramics formed using starch consolidation. *Key Eng Mater* 2002;**206–213**:1957–60.
9. Galassi C, Roncari E, Capiani C, Fabbri G, Piancastelli A, Peselli M, et al. Processing of porous PZT materials for underwater acoustics. *Ferroelectrics* 2002;**268**:47–52.
10. Kim JG, Sim JH, Cho WS. Preparation of porous (Ba,Sr)TiO_3 by adding corn-starch. *J Phys Chem Solids* 2002;**63**:2079–84.
11. Kim JG, Cho WS, Sim JH. Effect of potato-starch on the microstructure and PTCR characteristics of (Ba,Sr)TiO_3. *J Mater Sci: Mater Electron* 2002;**13**:497–501.
12. Díaz A, Hampshire S. Characterization of porous silicon nitride materials produced with starch. *J Eur Ceram Soc* 2004;**24**:413–9.
13. Mattern A, Huchler B, Staudenecker D, Oberacker R, Nagel A, Hoffmann MJ. Preparation of interpenetrating ceramic–metal composites. *J Eur Ceram Soc* 2004;**24**:3399–408.
14. Reynaud C, Thévenot F, Chartier T, Besson J-L. Mechanical properties and mechanical behaviour of SiC dense-porous laminates. *J Eur Ceram Soc* 2005;**25**:589–97.
15. Barea R, Osendi MI, Ferreira JMF, Miranzo P. Thermal conductivity of highly porous mullite material. *Acta Mater* 2005;**53**:3313–8.
16. Galassi C. Processing of porous ceramics—piezoelectric materials. *J Eur Ceram Soc* 2006;**26**:2951–8.
17. García-Gabaldón M, Pérez-Herranz V, Sánchez E, Mestre S. Effect of porosity on the effective electrical conductivity of different ceramic membranes used as separators in electrochemical reactors. *J Membrane Sci* 2006;**280**:536–44.
18. Romano P, Velasco FJ, Torralba JM, Candela N. Processing of M2 powder metallurgy high-speed steel by means of starch consolidation. *Mater Sci Eng A* 2006;**419**:1–7.
19. Gregorová E, Živcová Z, Pabst W. Porosity and pore space characteristics of starch-processed porous ceramics. *J Mater Sci* 2006;**41**:6119–22.
20. Gregorová E, Pabst W. Porosity and pore size control in starch consolidation casting—achievements and problems. *J Eur Ceram Soc* 2007;**27**:669–72.
21. Mao X, Wang S, Shimai S. Porous ceramics with tri-modal pores prepared by foaming and starch consolidation. *Ceram Int* 2008;**34**:107–12.
22. Živcová Z, Gregorová E, Pabst W, Smith DS, Michot A, Poulier C. Thermal conductivity of porous alumina ceramics prepared using starch as a pore-forming agent. *J Eur Ceram Soc* 2009;**29**:347–53.
23. Gregorová E, Živcová Z, Pabst W. Porous ceramics made using potato starch as a pore-forming agent. *Fruit, Veg Cereal Sci Biotechnol* 2009;**3**:115–27.
24. Živcová Z, Černý M, Pabst W, Gregorová E. Elastic properties of porous oxide ceramics prepared using starch as a pore-forming agent. *J Eur Ceram Soc* 2009;**29**:2765–71.
25. Gregorová E, Živcová Z, Pabst W. Starch as a pore-forming and body-forming agent in ceramic technology. *Starch/Stärke* 2009;**61**:495–502.
26. Živcová Z, Gregorová E, Pabst W. Low- and high-temperature processes and mechanisms in the preparation of porous ceramics via starch consolidation casting. *Starch/Stärke* 2010;**62**:3–10.
27. Gregorová E, Pabst W, Bohačenko I. Characterization of different starch types for their application in ceramic processing. *J Eur Ceram Soc* 2006;**26**:1301–9.
28. Dai Z. Starch granule size distribution in grains at different positions on the spike of wheat (Triticum aestivum L.). *Starch/Stärke* 2009;**61**:582–9.
29. Stephen AM, editor. *Food polysaccharides and their applications*. New York: Marcel Dekker; 1995. p. 19–67.
30. Macrae R, Robinson RK, Sadler MJ, editors. *Encyclopedia of food science, food technology and nutrition*. San Diego: Academic Press; 1993. p. 4372–90.
31. Belitz H-D, Grosch W, Schieberle P, editors. *Food chemistry*. 2nd ed. Berlin: Springer; 2004. p. 298–341.
32. Topin V, Radjaï F, Delenne J-Y, Mabille F. Mechanical modeling of wheat hardness and fragmentation. *Powder Technol* 2009;**190**:215–20.
33. Beyer H, Walter W [in German] *Lehrbuch der Organischen Chemie*. 20th ed. Stuttgart: S. Hirzel Verlag; 1984. p. 110–23, 420–33, 843–8.
34. Santacruz I, Rodrigues Neto JB, Moreno R. Preparation of cordierite materials with tailored porosity by gelcasting with polysaccharides. *Int J Appl Ceram Technol* 2008;**5**:74–83.
35. Gregg SJ, Sing KSW. *Adsorption, surface area and porosity*. 2nd ed. London: Academic Press; 1982. p. 173–94.
36. Saltykov SA [in German] *Stereometrische Metallographie*. Leipzig: VEB Deutscher Verlag für Grundstoffindustrie; 1974. p. 173–82.
37. Pabst W, Berthold C, Gregorová E. Size and shape characterization of polydisperse short-fiber systems. *J Eur Ceram Soc* 2006;**26**: 1121–30.
38. Talou MH, Villar MA, Camerucci MA. Thermogelling behaviour of starches to be used in ceramic consolidation processes. *Ceram Int* 2010;**36**:1017–26.
39. Trtík P, *Starch consolidation casting of alumina ceramics* [in Czech]. M.Sc. thesis. ICT Prague, Prague; 2005.
40. Gregorová E, Živcová Z, Pabst W, Sedlářová I. Characterization of porous ceramics by image analysis and mercury porosimetry. *Ceramika-Ceramics* 2006;**97**:219–30.
41. Prabhakaran K, Melkeri A, Gokhale NM, Sharma SC. Preparation of macroporous alumina ceramics using wheat particles as gelling and pore-forming agent. *Ceram Int* 2007;**33**:77–81.
42. He X, Zhou X, Su B. 3D interconnective porous alumina ceramics via direct protein foaming. *Mater Lett* 2009;**63**:830–2.
43. Gonzenbach UT, Studart AR, Steinlin D, Tervoort E, Gauckler LJ. Processing of particle-stabilized wet foams into porous ceramics. *J Am Ceram Soc* 2007;**90**:3407–14.